



Analysis of alternative measurement strategies for the inverse optimization of the hydraulic properties of a volcanic soil

A. Ritter^{a,*}, R. Muñoz-Carpena^b, C.M. Regalado^a, M. Vanclooster^c, S. Lambot^c

^a*Instituto Canario de Investigaciones Agrarias (ICIA), Apdo. 60, 38200 La Laguna (Tenerife), Spain*

^b*TREC-IFAS, Agricultural and Biological Engineering Department, University of Florida, 18905 SW 280 St., Homestead, FL 33031, USA*

^c*Department of Environmental Sciences and Land Use Planning, Unité Génie Rural, Université Catholique de Louvain, Croix du Sud, 2, BP2. B-1348 Louvain-la-Neuve, Belgium*

Received 26 November 2002; revised 26 February 2004; accepted 5 March 2004

Abstract

Data of two or more state variables are recommended for porous media flow parameter estimation by inverse modeling. In this context, it is desirable to minimize efforts and cost when measuring these variables. A method to analyze the suitability of different sampling alternatives to identify the flow parameters from transient flow experiments by inverse modeling is proposed and tested in a large undisturbed volcanic soil column. Alternative measurement strategies are defined by combining observed data from different hydraulic state variables with a variable depth resolution. The state variables considered are soil water content (θ), matric pressure head (h), and the water flux at the bottom of the soil column (q). The performance of the inverse analysis is measured by means of a factorial evaluation index, encompassing a measure of the goodness-of-fit and parameter uncertainty. To test this approach, two experiments were conducted where θ and h were measured at a maximum measurement depth frequency of seven observation depths per profile. A first irrigation experiment served to make an initial direct estimate of the flow parameters for the four soil horizons in the column. From this initial experiment, the hydraulic parameters selected for inverse estimation are reduced to the saturated water content and the van Genuchten's suction curve shape parameters. Results from the second transient irrigation experiment show that although inverse modeling using data from all the state variables considered (θ , h and q) give the best results, monitoring of θ in combination with either h or q proves to be sufficient, even when only four observation depths are considered.

© 2004 Elsevier B.V. All rights reserved.

Keywords: Canary Islands; Inverse modeling; Multilevel coordinate search; Parameter estimation; Volcanic soils; WAVE model

1. Introduction

Computer models of soil water and solute transport are nowadays widely used for assessing the impact of agricultural activities on groundwater resources and

for designing best management practices to reduce these impacts. This is the case in the Canary Islands (Spain), where appropriate agricultural and water management is needed for reducing the impacts of the intensive subtropical horticulture on the groundwater resources.

The success of modeling soil flow and transport processes heavily depends on the quality of the model

* Corresponding author.

E-mail address: aritter@icia.es (A. Ritter).

parameters that are used to describe the soil's hydraulic behavior (i.e. if they are representative of the soil transport and hydraulic properties). A complex and increasingly attractive form of parameter estimation is inverse modeling, since it (i) provides effective parameters in the range of envisaged model applications; (ii) allows for relatively simple experimental design, as few restrictions are imposed upon the experimental conditions; (iii) allows to determine simultaneously water retention and hydraulic conductivity functions; and (iv) can handle data from transient flow experiments, which are inherently faster than steady-state experiments (Si and Kachanoski, 2000; Zou et al., 2001; Section 3.6.2.1 in Dane and Topp, 2002). Using inverse modeling, parameters are optimized by minimizing a suitable objective function (OF) that expresses the discrepancy between the output of a numerical model and the observations of a certain hydraulic state variable (e.g. matric pressure head, soil water content, flow rates) (Si and Kachanoski, 2000). For this approach a global optimization algorithm can be coupled with a numerical forward flow model. Among such algorithms, the GMCS–NMS (Global Multilevel Coordinate Search combined with a Nelder Mead Simplex), described by Huyer and Neumaier (1999) and Lambot et al. (2002), is a powerful tool available.

However, the practical application of the inverse modeling approach faces some limitations related to parameter identifiability (i.e. when more than one parameter set lead to the same model response) and robustness of the algorithm. Moreover, the optimized parameters may be influenced by the boundary conditions and assumptions used in the procedure: e.g. dealing with a large number of parameters; fixing some of the parameters; the type of OF used; and the quality of the information contained in the measured variables to identify a unique parameter set. To overcome these limitations, several recommendations have been suggested such as modifying the experimental boundary conditions (Eching and Hopmans, 1993); constraining the parameter space by introducing prior parameter information (Russo et al., 1991; Abbaspour et al., 1999; Section 3.6.2.9 in Dane and Topp, 2002); reducing the experimental errors (Kool et al., 1985); improving the efficiency and robustness of the inversion algorithm (Kool et al., 1987); or introducing additional measurements of one or more

state variables (Kool and Parker, 1988; Eching and Hopmans, 1993; Section 3.6.2.9 in Dane and Topp, 2002). The usefulness of additional data may depend on its sensitivity to the hydraulic parameters, the independence of the existing observations, and the measurement error (Si and Kachanoski, 2000). In such a context, the effectiveness of different measurement alternatives for the inverse estimation of soil hydraulic properties needs to be analyzed in detail. This is an important issue, since some variables are easier to measure than others and are thus more suitable for inverse modeling (Abbaspour et al., 1999). Moreover, when designing an experiment, efforts and costs should be minimized. Decisions on sampling variables and methods should be based on quantitative and objective information rather than on intuition.

In this article, we present a procedure to analyze the suitability of different sampling alternatives (measurement strategies) to identify the flow parameters from transient flow experiments. The proposed method of analysis can be used at the experimental design stage using synthetic data obtained from a simulation run with reference parameters or for the estimation of flow properties from available 'observed' data. Alternative measurement strategies are considered combining different state variables at different sampling locations in the soil profile. To facilitate the evaluation of the alternative strategies, we introduce a factorial evaluation index (FEI) that integrates goodness-of-fit and parameter uncertainty. The analysis is applied to the estimation of the soil hydraulic parameters from irrigation experiments performed on a large undisturbed volcanic soil column. Matric pressure head, soil water content, and/or bottom flux data are introduced in the inversion problem. The parameters were inversely estimated using the water flow module of the WAVE model coupled with the GMCS combined sequentially with NMS algorithm (GMCS–NMS).

2. Materials and methods

2.1. The forward numerical model

To describe the flow in the unsaturated monolith, the one-dimensional computer code WAVE (Vanclouster et al., 1996) was used. The quality of the numerical solution of this model was recently

successfully tested in a numerical flow modeling benchmark exercise (Vanderborght et al., 2002). WAVE simulates transient flow by numerically solving the one-dimensional, isothermal Darcian flow equation in a variably saturated, rigid porous medium, using the mass-conservative scheme of Richards equation according to Celia et al. (1990):

$$C(h) \frac{\partial h}{\partial t} = \frac{\partial}{\partial z} \left[K(h) \left[\frac{\partial h}{\partial z} + 1 \right] \right] \quad (1)$$

where $C(h)$ is the soil water content capacity [L^{-1}]; z is the vertical distance from the soil surface [L], defined as positive upward; t is the time [T]; $K(h)$ is the hydraulic conductivity [LT^{-1}] and h is the matric pressure head [L]. It is worth noticing that Eq. (1) (h -based formulation) is appropriate in this study instead of the mixed formulation suggested by Celia et al. (1990), because of the high h values observed during the experiments herein.

The soil moisture retention curve is assumed to be of the form described by van Genuchten (1980):

$$S_e(h) = \frac{\theta(h) - \theta_r}{\theta_s - \theta_r} = [1 + (\alpha|h|)^n]^{-m} \quad (2)$$

where S_e is the effective saturation [$-$]; $\theta(h)$ is the soil water content [L^3L^{-3}] at matric pressure head h ; θ_s and θ_r are the saturated and residual soil water content [L^3L^{-3}], respectively; α is the inverse of the air entry value [L^{-1}]; m and n are curve shape parameters. The m characterizes the asymmetry, while the n is related to the slope of the curve (Vanclooster et al., 1996). Combining Eq. (2) with the pore-size distribution model of Mualem (1976) and using the constraint $m = 1 - 1/n$, yields an expression for the unsaturated hydraulic conductivity function (van Genuchten, 1980):

$$K(S_e) = K_s S_e^\lambda [1 - (1 - S_e^{1/m})^m]^2 \quad (3)$$

where $K(S_e)$ and K_s are the unsaturated and saturated hydraulic conductivity [LT^{-1}], respectively, and λ is the pore connectivity parameter [$-$], which accounts for tortuosity and correlation between pore sizes (Durner et al., 1999).

2.2. Inverse optimization procedure

2.2.1. Formulation of the inverse optimization problem

The inverse parameter estimation is formulated here as a nonlinear optimization problem, where the model's soil hydraulic parameters are optimized by minimizing a suitable OF based on the deviations between observed and predicted system response variables (Hopmans and Simunek, 1999; Section 3.6.2.2.b in Dane and Topp, 2002). The optimization process performed includes three basic steps repeated until some predefined convergence criteria are satisfied. These steps are: (i) parameter perturbation; (ii) forward modeling; and (iii) OF evaluation. In addition, an analysis of uncertainty is also performed. The formulation of the OF can be derived from the maximum likelihood theory that leads, under certain assumptions (Hopmans and Simunek, 1999), to a weighted least squares problem, taking the form:

$$\text{OF}(\mathbf{b}) = \sum_{j=1}^{n_v} \left\{ W_j \sum_{z=1}^{n_z} \sum_{i=1}^{n_j} w_{ij} [Y_j^*(z, t_i) - Y_j(z, t_i, \mathbf{b})]^2 \right\} \quad (4)$$

where the right-hand-side represents the deviations between the observed (Y^*) and the corresponding model-predicted (Y) space-time variable of type j (here matric pressure head, soil water content and bottom flux) using the soil hydraulic parameter set \mathbf{b} . n_j is the number of measurements over time within a particular set corresponding to the variable of type j , while n_v and n_z denote the number of different variables and observation depths, respectively. w_{ij} is the weight of a particular measurement, while W_j is a weighting factor that accounts for the differences between observation types due to different data set size (n_j), and is set equal to n_j^{-1} .

2.2.2. Global optimization algorithm

To minimize the OF, the WAVE model was coupled with the, GMCS, algorithm (Huyer and Neumaier, 1999). This algorithm combines global and local search capabilities with a multilevel approach. The GMCS is a good alternative to other existing optimization algorithms. It can deal with OFs with complex topography, it does not require powerful computing resources, and initial values of

the parameters to be optimized are not needed. In addition, for problems with finite bound constraints (parameter search space), the convergence is guaranteed if the OF is continuous in the neighborhood of the global minimum. Basically, using the GMCS, the parameter search space is split into smaller ‘boxes’. Each box is characterized by its midpoint, whose function value is known. A box can be split into smaller ones. As a rough measure of the numbers of times a box has been split, a so-called level is assigned to each box. The partitioning procedure is not uniform but parts where low OF values are expected are preferred. When the level of a box reaches a specified maximum value, the box is considered too small for further splitting and then, the local search relieves. These local enhancements are done via sequential quadratic programming and allow quickest convergence to the global minimum. To refine the minimization of the OF, the GMCS is combined sequentially with the NMS algorithm (Nelder and Mead, 1965). Further details about application of GMCS–NMS to inverse modeling of soil hydraulic properties are given in Lambot et al. (2002) and Ritter et al. (2003). Lambot et al. (2002) introduced the GMCS–NMS in the area of unsaturated hydrology and performed a positive evaluation of this algorithm in the identification of subsurface hydraulic properties from a continuously observed soil water content time series obtained from a numerical one-dimensional infiltration-redistribution experiment.

The available code that couples the GMCS–NMS algorithm with the WAVE model (Lambot et al., 2002) requires specific input files for each inverse optimization procedure, making multiple inverse simulations a tedious task. This code was modified for this study to allow for quicker and more flexible inverse procedures when combining different hydraulic variables and observation depths. Additional features added to the code were the uncertainty analysis and the evaluation of model performance described below, as well as facilities for running batch simulations and to export the results to spreadsheets.

2.2.3. Quantification of parameter uncertainty

Uncertainty associated with parameters estimated by inverse modeling is an essential aspect. Its quantification is built upon the following assumptions: (i) convergence to the global minimum; (ii) zero

model error; and (iii) independent and normally distributed residuals (measurement errors) (Hopmans and Simunek, 1999). However, as pointed out by Hollenbeck and Jensen (1998), parameter confidence regions are meaningless if adequacy is rejected. An ‘adequate’ model can explain the data to such a degree, that it can be reasonably assumed that the remaining discrepancy between predictions and observations are due to measurement errors. Thus, first we evaluated the model adequacy following the methodology proposed by these authors. If the OF (Eq. (4)) is normalized by setting the weights to $W_j = 1$ and $w_{i,j} = s_j^{-2}$ (where s_j denotes the measurement error), then the optimal sum-of-squares, $OF_{\min}(\mathbf{b}_{\text{opt}})$, follows a chi-square (χ^2) distribution with $N-P$ degrees of freedom (N is the number of data used to estimate the P parameters). Thereby, the probability of model adequacy (p_{adeq}) is computed from the χ^2 cumulative density function (cdf), Q , as:

$$p_{\text{adeq}} = 1 - Q[OF_{\min}(\mathbf{b}_{\text{opt}}), N - P] \quad (5)$$

According to Hollenbeck and Jensen (1998), $p_{\text{adeq}} > 0.5$ indicates that the model is ‘adequate’. Second, we obtained parameter confidence regions with the widely used approach based on the Cramer–Rao theorem and taking into account the suggestions of Hollenbeck and Jensen (1998) and Hollenbeck et al. (2000) as well. Details of this formulation can be found also elsewhere (Hopmans and Simunek, 1999; Kool and Parker, 1988; Lambot et al., 2002). Although this approach is restrictive and only approximately valid for nonlinear problems, it allows comparing confidence regions between parameters. Based on the Cramer–Rao theorem pseudo-univariate confidence limits are obtained as square roots of the diagonal elements ($C_{k,k}$) of the parameter variance–covariance matrix (because the confidence region is assumed to be an ellipsoid with its size proportional to the norm of the variance–covariance matrix). In addition, Hollenbeck and Jensen (1998) proposed a conservative way to express confidence regions based on projections of the confidence ellipsoid on the parameter axes. The confidence ellipsoid is defined via the maximum allowable change in the OF from its minimum, $\Delta OF(\mathbf{b})$. This follows a χ^2 distribution with P degrees of freedom. Consequently, for a desired level of confidence (p_{conf}), parameter confidence limits are

calculated as:

$$\xi_k^{\text{conf}} = \sqrt{Q^{-1}(p_{\text{conf}}, P)} \sqrt{C_{k,k}} \quad (6)$$

where ξ_k^{conf} is the confidence limit of parameter k , Q^{-1} is the inverse of the χ^2 cdf and $C_{k,k}$ is the diagonal elements of the parameter variance–covariance matrix corresponding to parameter k .

Hollenbeck and Jensen (1998) compared this approximate approach (exact only for linear models) with the exact method based on contouring the $\Delta\text{OF}(\mathbf{b})^{\text{conf}}$ for the whole parameter space. They remarked that the confidence regions (ellipsoids) obtained with both methods may differ (the higher p_{conf} , the larger is the discrepancy). In practice, however, it is difficult to compute $\Delta\text{OF}(\mathbf{b})$ for the whole discretized parameter space and determine for each one whether $\Delta\text{OF}(\mathbf{b})$ is larger or smaller than $\Delta\text{OF}(\mathbf{b})^{\text{conf}}$. Thus, it is recommended to use $p_{\text{conf}} = 90\%$ rather than 95% (Hollenbeck et al., 2000).

2.2.4. Sampling strategies for the inverse problem

We refer here to the term ‘strategy’ to denote a certain combination of measured data to be used for the inverse optimization of parameters. Each strategy implies a particular formulation of the OF according to the number and type of observations chosen. Thus, when considering only distinct types of measurements, seven different OFs (Eq. (4)) can be formulated by combining three hydraulic variables: (h), (θ), (q), ($h\theta$), (hq), (θq) and ($h\theta q$); where h , θ and q , represent matric pressure head, soil water content and bottom flux, respectively. On the other hand, using these combinations, more strategies can be obtained by taking into consideration different numbers of observation depths. Further in this article, we will use the notation $(\text{var})_L$ to identify the strategies; where var represents the combinations of hydraulic variables and L the number of observation depths.

The performance of several sampling strategies for the inverse optimization of hydraulic parameters was analyzed in two steps. First, we performed inverse modeling independently for each of the seven OFs mentioned above, considering that the readings from all observation depths were available. Secondly, once we evaluated which of those strategies were more appropriate, these were further tested by reducing the number of observation depths. Thereby, we verified if the same

inversion procedure performance was achieved with less observations points, i.e. lower experimental cost.

Several potential statistics are available to evaluate the performance of the inversion procedure. However, it is recommended to use the least number of statistics as possible (Wilson, 2001). In this context, Finsterle and Faybishenko (1999) suggested to use an aggregate measure of parameter uncertainty with a goodness-of-fit criterion. We quantified the model’s goodness-of-fit with the normalized mean square error ($n\text{MSE}$). This statistic is a measure of the variance about the 1:1 line compared to the variance of the observed data (s_o^2). The smaller the $n\text{MSE}$, the better the model predictions fit the observed data ($n\text{MSE} = 0$ corresponds to a perfect fit) (Wilson, 2001). The $n\text{MSE}$ for a j -type hydraulic variable was calculated as follows:

$$n\text{MSE}_j = \frac{\text{MSE}_j}{s_o^2} = \frac{\sum_{i=1}^{n_j} [Y_j^*(z, t_i) - Y_j(z, t_i, \mathbf{b})]^2}{\sum_{i=1}^{n_j} [Y_j^*(z, t_i) - \bar{Y}_j^*]^2} \quad (7)$$

Thereby, a $n\text{MSE}$ corresponding to the three observation types, $j = 1 \dots 3$ (matric pressure head, soil water content and bottom flux) was calculated for each strategy and considering the whole profile. On the other hand, uncertainty was taken into consideration by the 90% confidence limits calculated with Eq. (6). Non-dimensional ξ_k^{90} , relative to the estimated parameter value, were considered for each k -parameter and are denoted herein as ε_k^{90} . To make comparisons between strategies easier, we propose a FEI that combines both criteria (goodness-of-fit and uncertainty). The FEI takes into account that model performance is better when both, $n\text{MSE}$ and parameter uncertainty are small. We considered that the contribution of both criteria to the index is multiplicative, so that geometric means of components may be used (Limpert et al., 2001). In addition, we also include p_{adeq} in the FEI definition to account for model adequacy. Thereby, the FEI for each strategy was calculated as follows:

$$\text{FEI} = C \left[\prod_{k=1}^P \varepsilon_k^{90} \right]^{-1/P} \left[\prod_{j=1}^{n_v} n\text{MSE}_j \right]^{-1/n_v} \\ \times p_{\text{adeq}} H(p_{\text{adeq}} - 0.5) = C \frac{p_{\text{adeq}} H(p_{\text{adeq}} - 0.5)}{(\varepsilon_k^{90})_{\text{GM}} n\text{MSE}_{\text{GM}}} \quad (8)$$

where the subscript GM denotes the geometric mean among the j -type hydraulic variables considered ($n_v = 3$, for θ , h and q) or among the k -parameters ($P = 8$, as described below). C is a scaling constant to set the range of FEI values from 0 to 1 ($C = 2 \times 10^{-3}$ in our case). $H(p_{\text{adeq}} - 0.5)$ is the Heaviside step function (Abramowitz and Stegun, 1972, p. 1020) that cancels FEI if the model is not 'adequate'. Following FEI's definition, the better measurement strategies will be characterized by a higher FEI.

Finally, to determine whether alternative measurement strategies perform statistically different, significance tests were made on the $n\text{MSE}$'s (Steel et al., 1997).

2.3. Experimental set-up

A large monolith of undisturbed volcanic soil (sandy-clay-loam texture) was taken from a banana (*Musa accuminata* cv. 'Grande Naine') field in Tenerife (Canary Islands, Spain). The plantation was under a shadehouse and drip irrigated on a terraced banana field, typical in the Canary Islands, where it has sustained continuous cultivation for the last 20 years. Terraces are built by distributing a 70–90 cm thick layer of soil upon a drainage layer of fractured basaltic rock. Although the resulting soil profiles are initially homogeneous, intensive agricultural practices can result in the development of horizons in the soil profile. Changes in the water holding capacity can be attributed to organic matter incorporation to the soil (Vereecken et al., 1989), soil degradation due to saline water irrigation (Armas-Espinel et al., 2002), and surface compaction processes, which affect porosity (Dorel et al., 2000).

To reduce the effect of preferential flow along the walls during the irrigation experiments, large cylinders with big diameters are recommended (Schneider and Howell, 1991). A device was developed to extract large undisturbed soil columns in stainless steel cylinders ($\text{Ø}45 \times 85 \times 0.4$ cm thickness), based on an oil hydraulic press, which applied up to 66 kN pressure on a steel plate. The insertion plate was supported by a metallic structure that was anchored to the soil. The monolith was then brought to the laboratory, where it was instrumented with 21 TDR probes (three rods $\text{Ø}0.3 \times 20$ cm and 2.5 cm separation) and seven digital tensiometers

(tensiometric tube with porous ceramic and a pressure transducer) (Fig. 1), inserted at seven observation depths (denoted as A–G). At each depth (separated 10 cm apart on the vertical direction starting from the top), three TDR probes were inserted at 120° from each other. A collector, equipped with a pressure transducer, was used to measure the volume of water coming out from the base of the monolith during each experiment (bottom flux). All devices were multiplexed and connected to a PC. Monitoring the hydraulic variables was possible using a custom-made software (developed at I.T.A.C.L.-Valladolid, Spain).

A small rainfall-simulator was constructed to apply water uniformly at the top of the column using a $550 \times 550 \times 32$ mm³ plexi-glass box equipped with 310 hypodermic needles ($\text{Ø}0.3 \times 6$ mm spaced 20 mm apart). Water was pumped to the rainfall-simulator from a main container. On the bottom of the monolith, a constant-head boundary condition was imposed by using a 5 cm saturated sand bed (73 μm particle size), connected to a constant-level reservoir through a water-hose. A constant suction head was applied by setting the reservoir at a distance in the vertical direction from the bottom of the column, while continuity was maintained (Fig. 1).

2.4. Irrigation experiments

The laboratory experimental set-up allowed to perform irrigation experiments in an undisturbed soil column with controlled boundary conditions while monitoring different hydraulic variables. The top boundary condition consisted of irrigation applied homogeneously with the rainfall-simulator at the surface of the soil. To avoid soil dispersion, a 0.005 M CaSO_4 solution with thymol as a microbial inhibitor (Section 3.3.2.1.d in Dane and Topp, 2002) was used. To simplify we will refer to the latter as water. The bottom boundary was set at 10 cm suction, close to the average field values measured at that depth (Muñoz-Carpena, 1999).

Throughout each irrigation experiment, matric pressure head, soil water content and bottom flux were recorded at 15 min increments and then averaged at 1 h intervals. Although for some soils subjected to particular boundary conditions this may not be the case, averaging in time was possible here, because it

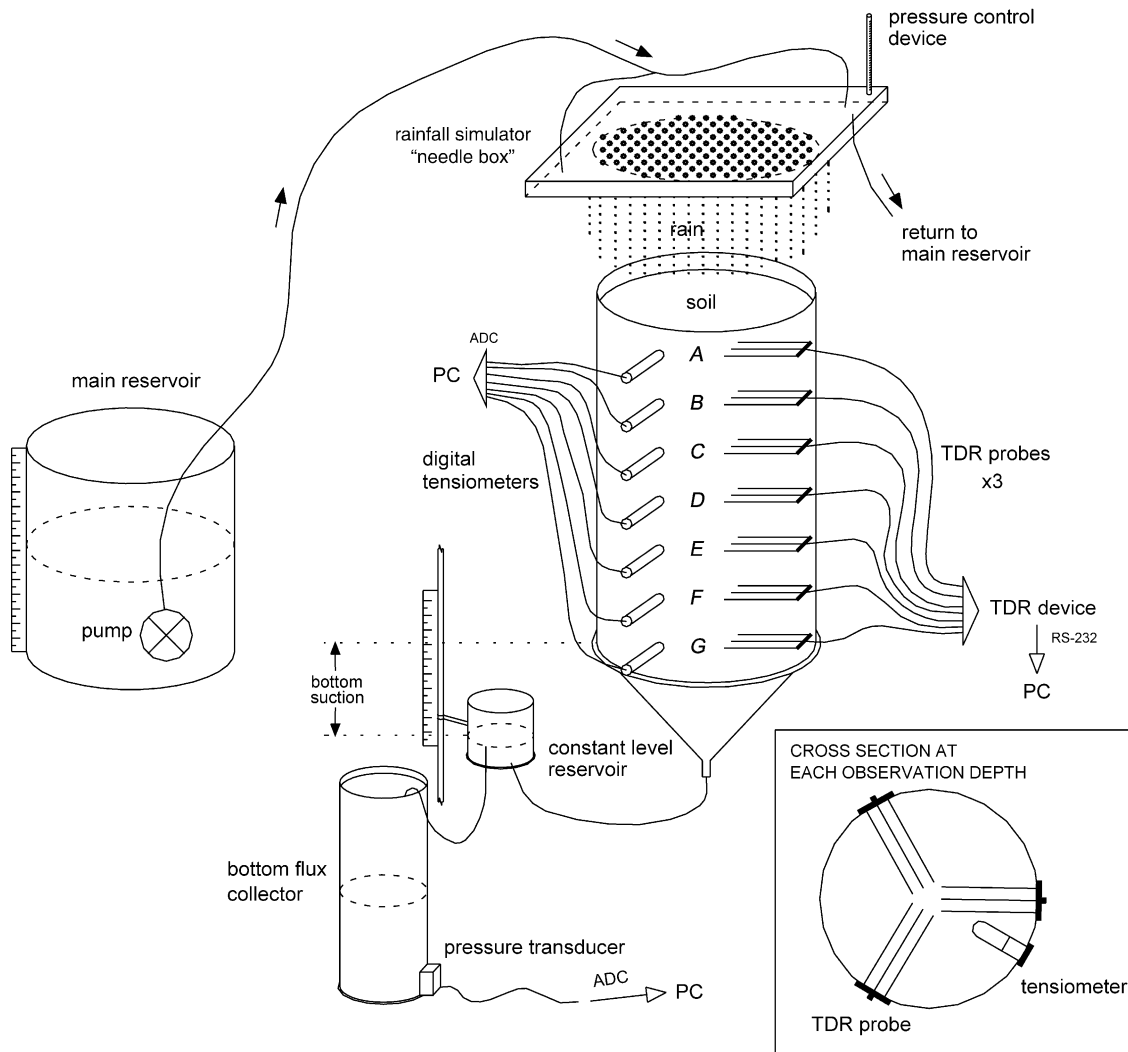


Fig. 1. Experimental set-up for irrigation experiments in the volcanic soil monolith.

did not imply strong curve smoothing. The sensor measurement error for the three variables (6.0 cm, $0.01 \text{ cm}^3 \text{ cm}^{-3}$ and 0.5 mm for pressure head, soil water content and volume of water collected at the bottom of the monolith, respectively) was estimated from calibration and transducer specifications.

The soil water content was estimated using a specific TDR-calibration for the same soil used in this study (Regalado et al., 2003). Soil water content at each time and depth was obtained by averaging the values measured with the three TDR probes at each of the seven depths.

A first irrigation experiment was performed to obtain information about the water retention in the soil profile. Starting from near saturated conditions, the monolith was continuously irrigated at different flow rates. The flux was reduced in four steps (5 mm/h during 94 h; 2.7 mm/h during 32 h; 1 mm/h during 41 h, and 0.2 mm/h during 72 h). Afterwards, irrigation was stopped and measurements continued until the soil profile reached hydraulic equilibrium (271 h). By using distinct flow rates it was possible to monitor the hydraulic variables at different moisture conditions. Plotting soil water content versus matric

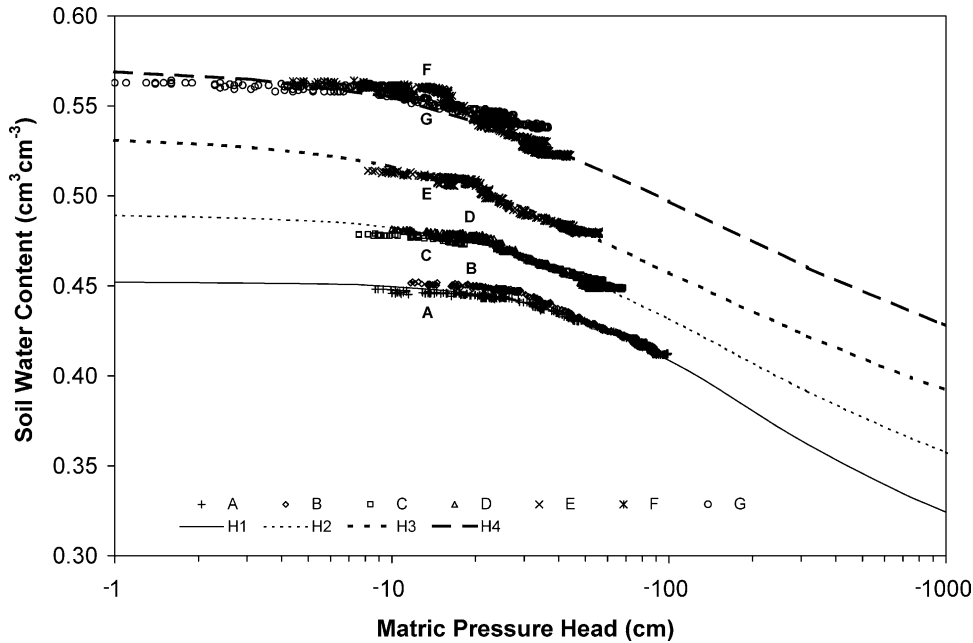


Fig. 2. Soil moisture retention curves observed in the monolith. Measured data (symbols) and fitted van Genuchten curves (lines).

pressure head data provided information about the water retention curve at the observation depths. Furthermore, these data, fitted to van Genuchten's curve with the RETC code (van Genuchten et al., 1991), provided an initial estimate of the hydraulic parameters in the optimization process.

A second transient irrigation experiment was carried out to obtain data for the inverse optimization of the hydraulic parameters. Four equal 5-l irrigations were applied at a rate of approximately 5.25 mm/h. Each one took around 6 h, while the time between irrigations was 18, 65 and 18 h.

Data corresponding to the first two irrigations of the second experiment were used for calibration, while the rest of the data set served for validation.

3. Results and discussion

Water retention data at each soil depth obtained from the first irrigation experiment was helpful to select the parameters to be optimized by inverse modeling with the second experiment. The first experiment suggested heterogeneities in the soil profile, where four horizons (H1–H4) with different water retention could be identified (Fig. 2). Table 1 shows the hydraulic parameters for those horizons. θ_r was fixed to an average value of 0.268, which results from measurements ranging between 0.219 and 0.330 (showing no significant differences at level 0.05). These were obtained for the same experimental plot by Armas-Espinel et al. (2002) at 15 cm and by

Table 1
Initial values of the hydraulic parameters based on first outflow experiment (Fig. 2)

Horizon	Observation depths	Depth (cm)	K_s (cm/h)	θ_s ($\text{cm}^3 \text{cm}^{-3}$)	α (cm^{-1})	n	R^2
H1	A,B	0–25.5	2.5	0.452	0.0120	1.473	0.9856
H2	C,D	25.5–45.0	15.0	0.489	0.0223	1.290	0.9631
H3	E	45.0–54.0	20.0	0.531	0.0489	1.193	0.9714
H4	F,G	54.0–72.0	30.0	0.569	0.0454	1.166	0.7667

θ_r was fixed to 0.268 for the four horizons.

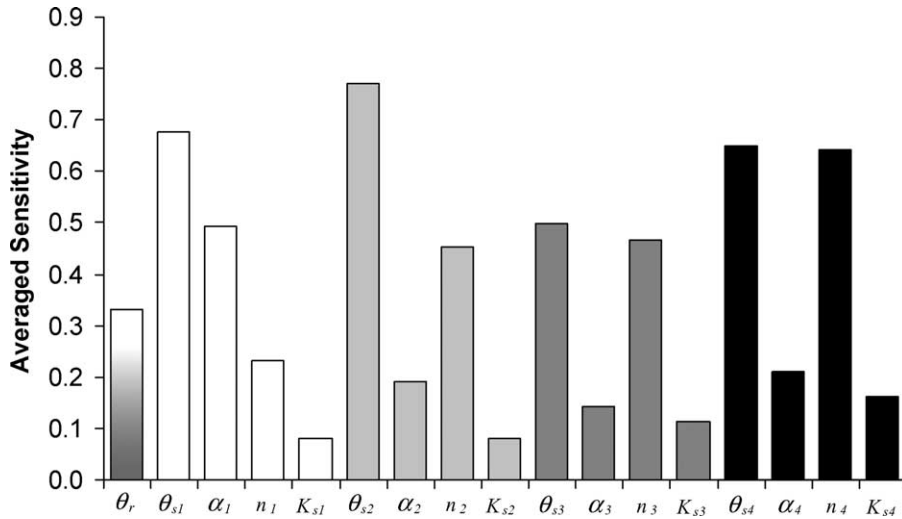


Fig. 3. Averaged sensitivity for the van Genuchten parameters of Table 2.

Muñoz-Carpena (1999) at 15, 30 and 60 cm depth. It is worth noticing that the large values of θ_r are typical of volcanic soils with strong natural micro-aggregation (Maeda et al., 1977).

A small experimental range of soil water content and matric pressure head was obtained and used for the inverse method. Although small, these ranges match those observed in the drip-irrigated banana plantation in this soil during normal conditions (Muñoz-Carpena, 1999). Therefore, under this high frequency irrigation technique, hydraulic properties near saturation are most important (Durner et al., 1999).

Inverse optimization of all the hydraulic parameters with the suggested algorithms is impractical when working with four distinct horizons, since the number of parameters that describe the hydraulic functions increased four-fold up to 24 parameters (i.e. θ_s , θ_r , α , n , K_s and λ for each of the four horizons). To reduce the number of parameters to be optimized, first $\lambda = 0.5$ was assumed (Mualem, 1976). Secondly, the selection of the other parameters to optimize by the inverse procedure was based on a sensitivity analysis. Thereby, the sensitivity of the three model outputs (water content, matric pressure head and bottom flux) to the parameters of Table 1 was evaluated by calculating relative sensitivity coefficients according to Yeh (1986) and Haan et al. (1982). In addition, time-averaged coefficients were obtained following Inoue et al. (1998). Results showed that soil water content

was mainly sensitive to the four saturated water contents, while matric pressure head was more sensitive to θ_{s2} , n_2 , n_3 , and n_4 . The bottom flux was also sensitive to these parameters and to α_1 as well. Finally, we averaged the sensitivity coefficients among the three state variables (Fig. 3). According to Fig. 3 we chose θ_{s1} , θ_{s2} , θ_{s3} , θ_{s4} , α_1 , n_2 , n_3 , and n_4 for optimization. Thus, a total of eight parameters were selected. Intervals delimiting the parameter search space for GMCS were set at [0.40–0.65] for θ_s ($\text{cm}^3\text{cm}^{-3}$) (according to Fig. 2); [1.05–1.60] for n and [0.005–0.050] for α_1 (cm^{-1}) (according to the range that corresponds to USDA soil fine textures reported by Carsel and Parrish, 1988). The other fixed

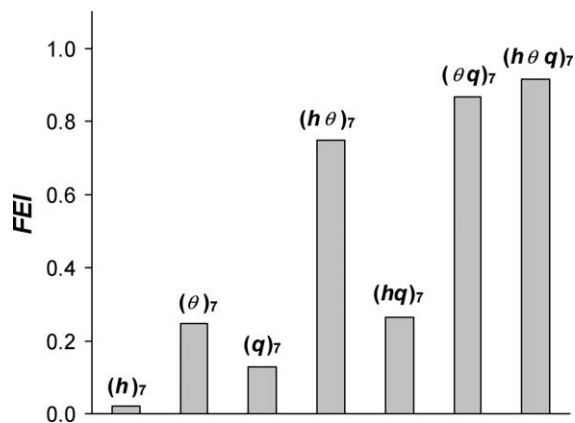


Fig. 4. Comparison of strategies (var)₇ based on the proposed FEI.

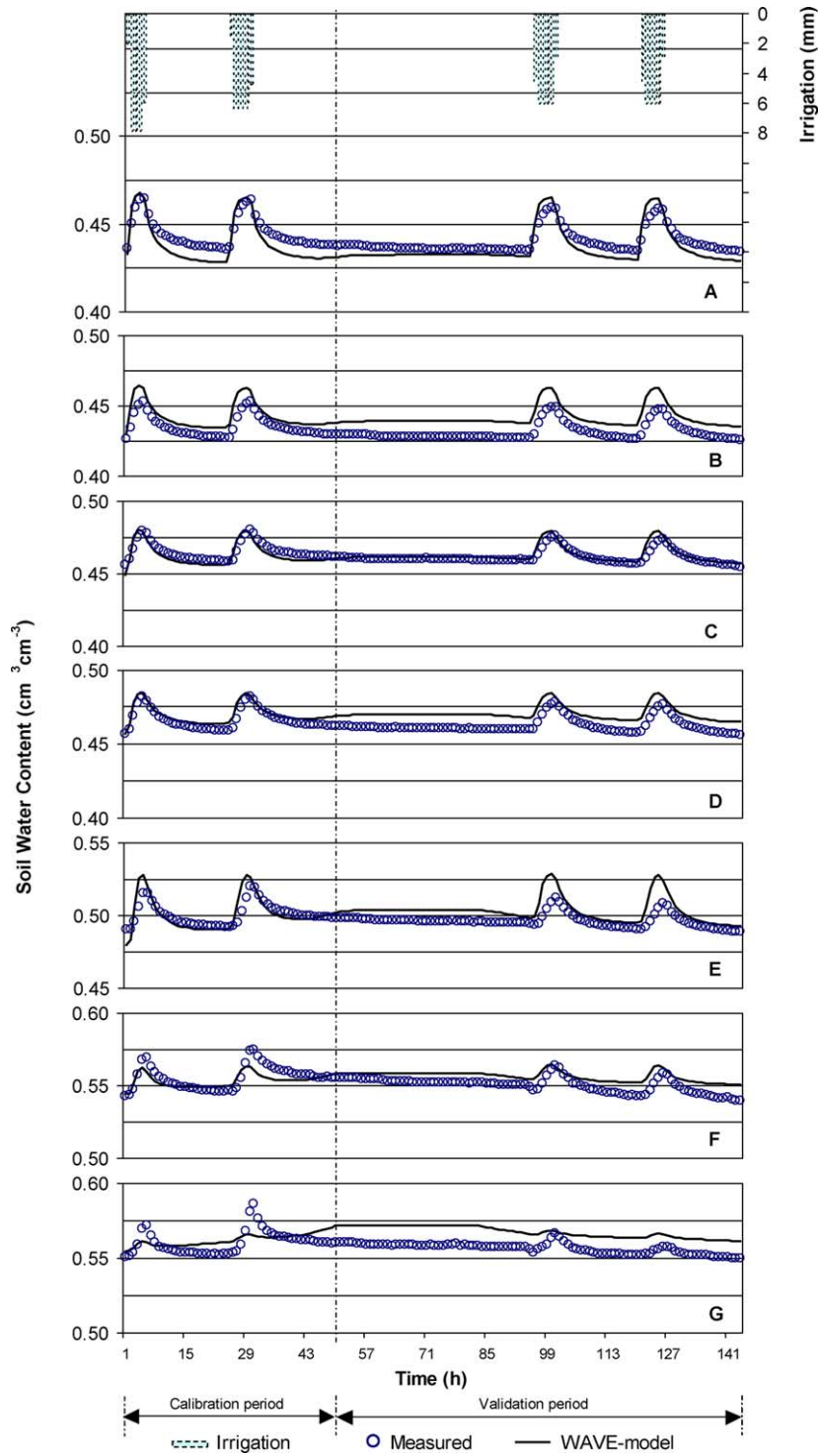


Fig. 5. WAVE model fit to soil water content data corresponding to $(h\theta)_7$.

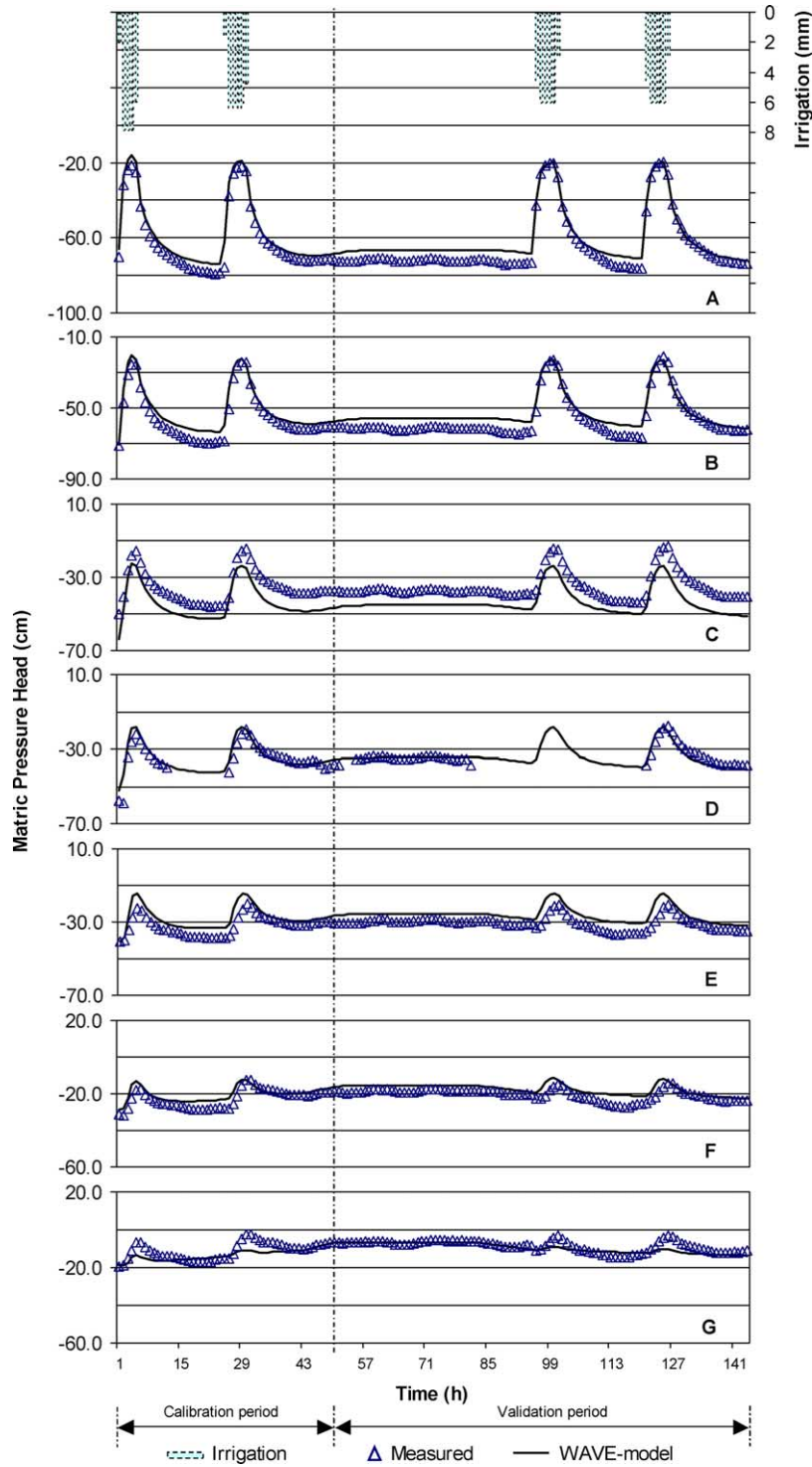


Fig. 6. WAVE model fit to matric pressure head data corresponding to $(h\theta)_7$.

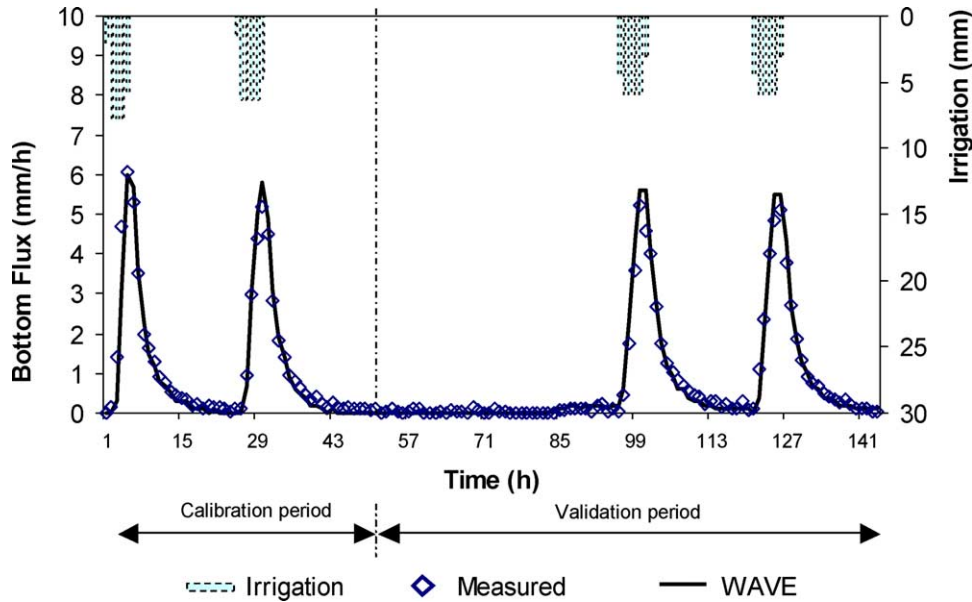


Fig. 7. WAVE model fit to bottom flux data corresponding to $(h\theta)_7$.

hydraulic parameters needed in the model were set to the values of Table 1. Although it is frequently recommended not to fix K_s at an independently measured value (Section 3.6.2.3.c in Dane and Topp, 2002), the sensitivity for this parameter was low (Fig. 3). Thus, we took for each horizon a K_s value estimated from the first irrigation experiment (Table 1).

Calculated FEI values (Fig. 4) show strategies $(h\theta q)_7$, $(\theta q)_7$, and $(h\theta)_7$ to be the best (highest index, respectively). As expected, including all information available in the OF, i.e. $(h\theta q)_7$, leads to best

results. The optimized parameters using $(h\theta q)_7$ were: $\theta_{s1} = 47.64 \pm 0.30\%$, $\theta_{s2} = 49.95 \pm 0.38\%$, $\theta_{s3} = 54.05 \pm 0.64\%$, $\theta_{s4} = 59.00 \pm 0.47\%$, $\alpha_{s1} = 0.0172 \pm 0.0004 \text{ cm}^{-1}$, $n_2 = 1.385 \pm 0.066$, $n_3 = 1.228 \pm 0.029$, and $n_4 = 1.244 \pm 0.031$. We conclude thereby, the adequacy of using soil water content data combined with other hydraulic variables (e.g. matric pressure head or bottom flux).

The evaluation of the strategies was also complemented by visual inspection of simulated versus observed data. From the seven strategies only the three above-mentioned showed a satisfactory fit.

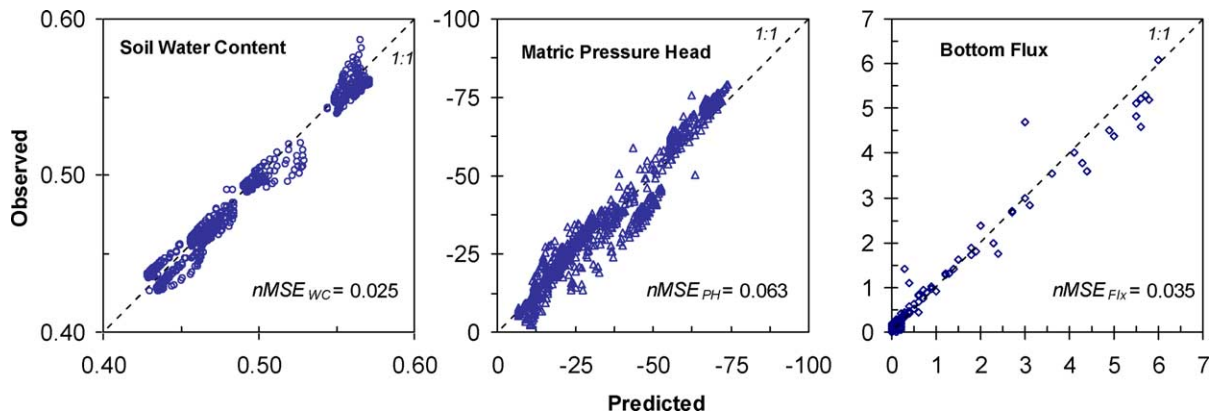


Fig. 8. Goodness of fit between observed and simulated values with $(h\theta)_7$.

As an example, Figs. 5–7 show model performance using $(h\theta)_7$ for soil water content and matric pressure head at the seven monitoring depths, and for bottom flux as well. Furthermore, agreement between observed and predicted data for the three hydraulic variables is presented in Fig. 8. From these figures, we conclude that model predictions were generally satisfactory.

In this context, Simunek and van Genuchten (1996) obtained best parameter identifiability when both pressure head and soil water content were used simultaneously. In a study on two homogeneous soils, Abbaspour et al. (1999) compared the unsaturated hydraulic properties obtained by inverse methods using different combinations of measured variables (among pressure head, soil water content and cumulative discharge) in the OF. Based on the MSE, they did not find statistical differences in the results obtained with the distinct formulations of the OF. Keeping in mind that we are interested in finding a suitable strategy (i.e. best results with lower costs), we tested if those strategies were statistically different. No significant differences (at level 0.05) were found between the $nMSE$'s corresponding to $(h\theta)_7$, $(\theta q)_7$ and $(h\theta q)_7$.

Based on our previous results, we used the best alternatives $[(h\theta)_L, (\theta q)_L$ and $(h\theta q)_L]$ to test if reducing the number of measurement points (depths) would lead to acceptable results. First, we chose four observation depths (one per horizon) trying two different combinations of them: $(var)_4''\{ACEG\}$ and $(var)_4''\{BDEF\}$. Second, combinations of three depths were considered to check if three observation depths would still have enough information for the parameter estimation of the four horizons: $(var)_3''\{ADG\}$, $(var)_3''\{AEG\}$ and $(var)_3''\{BCF\}$.

The FEI values for the six combinations and the three alternatives are presented in Fig. 9. First, $(var)_3$ implied an important reduction of the FEI. Therefore, strategies with less than 4 observation depths are not recommended. Second, when using four observation depths, $(var)_4'$ and $(var)_4''$, a decrease in the calculated FEI was observed, too. Finally, no significant differences (at level 0.05) were found between $(var)_7$ and $(var)_4$. The estimated parameters obtained with each strategy are presented in Table 2.

Based on all this, measuring at only four depths (one per horizon) would be sufficient if soil water content data and either matric pressure head or bottom

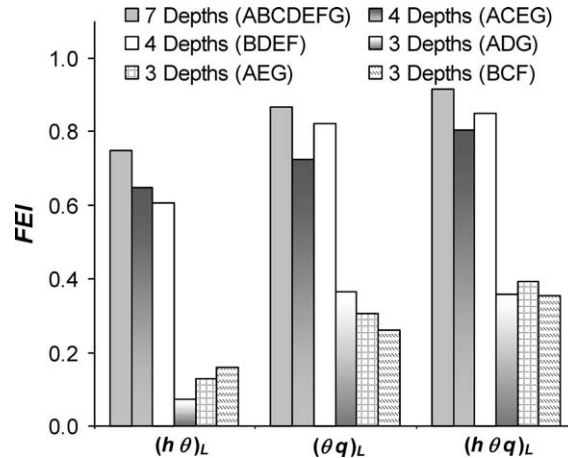


Fig. 9. Comparison of strategies $(h\theta)_L$, $(\theta q)_L$ and $(h\theta q)_L$ based on the proposed FEI.

flux are used. From a practical point of view (lower cost, simplicity), using soil water content and suction readings at only four depths, i.e. $(h\theta)_4$, is desirable. In this context, despite the higher cost of using suction readings (digital tensiometers) when compared to monitoring bottom flux, they have the added benefit of providing information about the soil water retention curve. In addition, bottom flux measurements are in most cases impractical in a field situation, so h and θ (tensiometers and TDR) would be preferred.

4. Summary and conclusions

The suitability of alternative soil water flow monitoring strategies for the inverse estimation of the soil hydraulic parameters of a volcanic soil is analyzed. Inverse modeling is performed by coupling the GMCS–NMS algorithm to the flow module of the WAVE model. Use is made of experimental data collected during two irrigation experiments conducted in a large undisturbed soil column. The results from the first experiment reveal the existence of four well-defined soil horizons with different water retention curves. Using these results and a sensitivity analysis, the hydraulic parameters selected for inverse modeling are reduced to eight (saturated water content, θ_s , in the four horizons, and the curve shape parameters: α in the first horizon, and n in the three other horizons). Inverse optimization of these properties is successful

Table 2
 Estimated soil hydraulic parameters and ξ_k^{90} for all strategies

Strategy	$\theta_{s1}(\%)$	$\theta_{s2}(\%)$	$\theta_{s3}(\%)$	$\theta_{s4}(\%)$	$\alpha_l(\text{cm}^{-1})$	$n_2(-)$	$n_3(-)$	$n_4(-)$
<i>ABCDEFG</i>								
$(h)_7$	48.73 ± 1.87	45.59 ± 7.08	72.60 ± 24.09	65.00 ± 12.76	0.0147 ± 0.0023	1.239 ± 0.064	1.848 ± 0.484	1.190 ± 0.056
$(\theta)_7$	46.20 ± 0.51	48.55 ± 0.77	53.30 ± 1.37	56.89 ± 0.71	0.0111 ± 0.0020	1.208 ± 0.087	1.191 ± 0.077	1.084 ± 0.045
$(q)_7$	40.12 ± 1.58	58.92 ± 1.20	48.29 ± 1.64	59.88 ± 0.55	0.0187 ± 0.0008	1.610 ± 0.061	1.398 ± 0.059	1.225 ± 0.041
$(h\theta)_7$	47.57 ± 0.35	49.96 ± 0.38	56.39 ± 0.93	58.18 ± 0.45	0.0157 ± 0.0005	1.344 ± 0.062	1.358 ± 0.037	1.173 ± 0.035
$(hq)_7$	43.08 ± 0.85	53.57 ± 1.35	63.20 ± 1.91	61.17 ± 0.39	0.0129 ± 0.0004	1.835 ± 0.051	1.172 ± 0.020	1.496 ± 0.034
$(\theta q)_7$	46.94 ± 0.31	51.10 ± 0.35	54.99 ± 0.63	59.21 ± 0.44	0.0144 ± 0.0003	1.536 ± 0.060	1.282 ± 0.029	1.257 ± 0.029
$(h\theta q)_7$	47.64 ± 0.30	49.95 ± 0.38	54.05 ± 0.64	59.00 ± 0.47	0.0172 ± 0.0004	1.385 ± 0.066	1.228 ± 0.029	1.244 ± 0.031
<i>ACEG</i>								
$(h\theta)_4'$	48.01 ± 0.41	49.71 ± 0.53	54.91 ± 0.57	57.83 ± 0.48	0.0150 ± 0.0006	1.300 ± 0.042	1.271 ± 0.046	1.161 ± 0.043
$(\theta q)_4'$	47.68 ± 0.45	52.04 ± 0.43	56.81 ± 0.54	59.47 ± 0.53	0.0155 ± 0.0005	1.581 ± 0.049	1.372 ± 0.055	1.317 ± 0.029
$(h\theta q)_4'$	47.28 ± 0.45	51.70 ± 0.51	54.94 ± 0.45	58.75 ± 0.44	0.0145 ± 0.0005	1.559 ± 0.044	1.267 ± 0.043	1.254 ± 0.043
<i>BDEF</i>								
$(h\theta)_4''$	47.88 ± 0.46	51.12 ± 0.85	56.98 ± 0.66	60.69 ± 0.56	0.0192 ± 0.0008	1.582 ± 0.044	1.368 ± 0.031	1.320 ± 0.040
$(\theta q)_4''$	47.29 ± 0.35	51.05 ± 0.42	55.90 ± 0.50	62.92 ± 0.54	0.0176 ± 0.0005	1.600 ± 0.034	1.309 ± 0.027	1.489 ± 0.037
$(h\theta q)_4''$	47.37 ± 0.34	51.30 ± 0.46	57.71 ± 0.74	63.74 ± 0.33	0.0181 ± 0.0004	1.611 ± 0.054	1.396 ± 0.035	1.549 ± 0.032
<i>ADG</i>								
$(h\theta)_3'$	48.00 ± 0.50	50.39 ± 0.93	72.96 ± 7.39	57.72 ± 0.41	0.0144 ± 0.0015	1.474 ± 0.173	1.715 ± 0.242	1.152 ± 0.030
$(\theta q)_3'$	46.61 ± 0.36	51.70 ± 0.40	58.70 ± 2.69	58.08 ± 0.40	0.0094 ± 0.0003	1.762 ± 0.042	1.820 ± 0.147	1.178 ± 0.019
$(h\theta q)_3'$	47.19 ± 0.34	50.47 ± 0.42	55.62 ± 3.59	58.03 ± 0.39	0.0115 ± 0.0003	1.498 ± 0.030	1.969 ± 0.131	1.151 ± 0.016
<i>AEG</i>								
$(h\theta)_3''$	48.16 ± 0.55	56.08 ± 3.34	57.33 ± 2.21	58.59 ± 0.45	0.0147 ± 0.0016	2.021 ± 0.389	1.395 ± 0.126	1.242 ± 0.069
$(\theta q)_3''$	47.99 ± 0.37	48.54 ± 1.78	54.32 ± 3.61	58.35 ± 0.40	0.0144 ± 0.0003	1.692 ± 0.046	1.235 ± 0.083	1.194 ± 0.026
$(h\theta q)_3''$	48.07 ± 0.38	49.40 ± 0.96	56.40 ± 1.72	58.63 ± 0.46	0.0144 ± 0.0004	1.777 ± 0.048	1.340 ± 0.084	1.232 ± 0.031
<i>BCF</i>								
$(h\theta)_3'''$	46.60 ± 0.84	50.62 ± 1.18	55.14 ± 5.51	58.54 ± 1.43	0.0156 ± 0.0032	1.426 ± 0.151	1.146 ± 0.052	1.181 ± 0.083
$(\theta q)_3'''$	47.15 ± 0.44	51.76 ± 0.65	54.54 ± 3.85	64.02 ± 0.79	0.0176 ± 0.0005	1.518 ± 0.069	1.293 ± 0.046	1.581 ± 0.060
$(h\theta q)_3'''$	47.01 ± 0.66	50.38 ± 0.58	51.06 ± 2.71	63.33 ± 0.69	0.0191 ± 0.0006	1.395 ± 0.038	1.138 ± 0.026	1.515 ± 0.042

using different monitoring strategies. The alternative strategies are based on the consideration of different hydraulic state variables and observation depths for the formulation of the OF. Furthermore, by defining an integrated index to account for different evaluation criteria, the best strategies are easily identified. Although inverse modeling using simultaneously soil water content (θ), matric pressure head (h), and bottom flux (q) data give the best results, monitoring of θ in combination with either h or q proves to be sufficient, even if only four observation depths are considered. It must be noticed that, despite the higher cost of using suction readings (digital tensiometers) when compared to the monitoring of the bottom flux, they have the added benefit of providing direct information about the soil water retention curve. Thereby, if low cost bottom flux measurements are chosen, additional methods or surveys (e.g. profile description) might be needed to obtain prior information for the inverse procedure.

Using synthetic data, based on estimated reference parameters, the procedure presented here may serve as a general method for assessing, at the experimental design stage, appropriate strategies to estimate the soil hydraulic parameters by inverse modeling. Since decisions about the type and number of observations required for inverse optimization are usually based on intuition, the procedure applied in this study represents an objective way to base such decisions on quantitative information.

Acknowledgements

Authors want to thank J. Álvarez-Benedí (I.T.A.C.L., Valladolid) for developing the data acquisition software used, and Martin Morawietz (University of Friburg) during the preparation of the experimental set-up. This work was financed with funds of the INIA-Plan Nacional de I + D Agrario (Proyecto I + D SC99-024-C2) and Dirección Gral. de Universidades e Investigación de la Consejería de Educación Cultura y Deportes del Gobierno de Canarias of Spain. M. Vanclouster and S. Lambot acknowledge the FNRS and the FRIA in Belgium for developing the modeling and inversion tools. This research was supported by the Florida Agricultural

Experiment Station (USA), and approved for publication as Journal Series No. R-09169.

References

- Abramowitz, M., Stegun, I.A. (Eds.), 1972. Handbook of Mathematical Functions with Formulas, Graphs, and Mathematical Tables, 9th printing, Dover, New York, p. 1046.
- Abbaspour, K.C., Sonnleitner, M.A., Schulin, R., 1999. Uncertainty in estimation of soil hydraulic parameters by inverse modeling: example lysimeter experiments. *Soil Sci. Soc. Am. J.* 63, 501–509.
- Armas-Espinel, S., Hernández-Moreno, J.M., Muñoz-Carpena, R., Regalado, C.M., 2002. Physical properties of sorriba cultivated volcanic soils from Tenerife in relation to diagnostic Andic parameters. *Geoderma* 117(3–4), 297–311.
- Carsel, R.F., Parrish, R.S., 1988. Developing joint probability distributions of soil water retention characteristics. *Water Resour. Res.* 24(5), 769–775.
- Celia, M.A., Bouloutas, E.T., Zarba, R.L., 1990. A general mass-conservative numerical solution for the unsaturated flow equation. *Water Resour. Res.* 26, 1483–1496.
- Dane, J.H., Topp, G.C., 2002. Methods of soils analysis. Part 4. SSSA Book Series, vol. 5., p. 1692.
- Dorel, M., Roger-Estrate, J., Manichon, H., Devaux, B., 2000. Porosity and soil water properties of Caribbean volcanic ash soils. *Soil Use Manage.* 16, 133–145.
- Durner, W., Schultze, B., Zurmühl, T., 1999. State-of-the-art in inverse modeling of inflow/outflow experiments. In: van Genuchten, M. Th., Leij, F.J., Wu, L. (Eds.), Proceedings of International Workshop, Characterization and Measurement of the Hydraulic Properties of Unsaturated Porous Media, University of California, Riverside, CA, pp. 713–724.
- Eching, S.O., Hopmans, J.W., 1993. Optimization of hydraulic functions from transient outflow and soil water pressure data. *Soil Sci. Soc. Am. J.* 57, 1167–1175.
- Finsterle, S., Faybishenko, B., 1999. Inverse modeling of a radial multistep outflow experiment for determining unsaturated hydraulic properties. *Adv. Water Resour.* 22(5), 431–444.
- Haan, C.T., Johnson, H.P., Brakensiek, D.L., Hydrologic Modeling of Small Watersheds. ASAE Monograph 5. St Joseph, ASAE, 1982.
- Hollenbeck, K.J., Jensen, K.H., 1998. Maximum-likelihood estimation of unsaturated hydraulic parameters. *J. Hydrol.* 210, 192–205.
- Hollenbeck, K.J., Simunek, J., van Genuchten, M.Th., 2000. RETMCL: Incorporating maximum likelihood estimation principles in the RETC soil hydraulic parameter estimation code. *Comput. Geosci.* 26, 319–327.
- Hopmans, J.W., Simunek, J., 1999. Review of inverse estimation of soil hydraulic properties. In: van Genuchten, M. Th., Leij, F.J., Wu, L. (Eds.), Proceedings of International Workshop, Characterization and Measurement of the Hydraulic Properties of Unsaturated Porous Media, University of California, Riverside, CA, pp. 713–724.

- Huyer, W., Neumaier, A., 1999. Global optimization by multilevel coordinate search. *J. Global Optim.* 14, 331–355.
- Inoue, M., Simunek, J., Hopmans, J.W., Clausnitzer, V., 1998. In situ estimation of soil hydraulic functions using a multistep soil-water extraction technique. *Water Resour. Res.* 34(5), 1035–1050.
- Kool, J.B., Parker, J.C., 1988. Analysis of the inverse problem for transient unsaturated flow. *Water Resour. Res.* 24, 817–830.
- Kool, J.B., Parker, J.C., van Genuchten, M.Th., 1985. Determining soil hydraulic properties from one-step outflow experiments by parameter identification: I. Theory and numerical studies. *Soil Sci. Soc. Am. J.* 49, 1348–1354.
- Kool, J.B., Parker, J.C., van Genuchten, M.Th., 1987. Parameter estimation for unsaturated flow and transport models—A review. *J. Hydrol.* 91, 255–293.
- Lambot, S., Javaux, M., Hupet, F., Vanclooster, M., 2002. A Global Multilevel Coordinate Search procedure for estimating the unsaturated soil hydraulic properties. *Water Resour. Res.* 38(11), 6/1–6/15.
- Limpert, E., Stahel, W.A., Abbt, M., 2001. Log-normal distributions across the sciences: keys and clues. *Bioscience* 51(5), 341–352.
- Maeda, T., Takenaka, H., Warkentin, B.P., 1977. Physical properties of allophane soils. *Adv. Agronom.* 29, 229–264.
- Muñoz-Carpena, R., 1999. Estudio de la Integración a Diferentes Escalas del Transporte de Aguas y Solutos en Suelos-IDEASS. Annual Project Report: SC99-024-C2-1 (in Spanish). INIA, Madrid.
- Mualem, Y., 1976. A new model for predicting the hydraulic conductivity of unsaturated porous media. *Water Resour. Res.* 12, 513–522.
- Nelder, J.A., Mead, R., 1965. A simplex method for function minimization. *Comput. J.* 7, 308–313.
- Regalado, C.M., Muñoz-Carpena, R., Socorro, A.R., Hernández-Moreno, J.M., 2003. Time domain reflectometry models as a tool to understand the dielectric response of volcanic soils. *Geoderma* 117(3–4), 313–330.
- Ritter, A., Hupet, F., Muñoz-Carpena, R., Lambot, S., Vanclooster, M., 2003. Using inverse methods for estimating soil hydraulic properties from field data as an alternative to direct methods. *Agric. Water Manage.* 59, 77–96.
- Russo, D., Bresler, E., Shani, U., Parker, J.C., 1991. Analyses of infiltration events in relation to determining soil hydraulic properties by inverse problem methodology. *Water Resour. Res.* 27(6), 1361–1373.
- Schneider, A.D., Howell, T.A., 1991. Large, monolithic, weighing lysimeters. In: Allen, R.G., et al. (Eds.), *Lysimeters for Evapotranspiration and Environmental Measurements*, Proceedings of the International Symposium on Lysimetry. ASCE, pp. 37–45.
- Si, B.C., Kachanoski, R.G., 2000. Estimating soil hydraulic properties during constant flux infiltration: inverse procedures. *Soil Sci. Soc. Am. J.* 64, 439–449.
- Simunek, J., van Genuchten, M.Th., 1996. Estimating unsaturated soil hydraulic properties from tension disc infiltrometer data by numerical inversion. *Water Resour. Res.* 32(9), 2683–2696.
- Steel, R.G.D., Torrie, J.H., Dickey, D.A., 1997. *Principles and Procedures of Statistics: A Biometrical Approach*, McGraw-Hill, New York, pp. 666.
- van Genuchten, M.Th., 1980. A closed-form equation for predicting the hydraulic conductivity of soil. *Soil Sci. Soc. Am. J.* 44, 892–898.
- van Genuchten, M.Th., Leij, F.J., Yates, S.R., 1991. *The RETC Code for Quantifying the Hydraulic Functions of Unsaturated Soils*, US Salinity Laboratory, CA, p. 85.
- Vanclooster, M., Viaene, P., Christiaens, K., Ducheyne, S., 1996. *Reference and User's Manual (release 2.1), vol. 1*. Institute for Land and Water Management, Katholieke Universiteit Leuven, Leuven, Belgium.
- Vanderborght, J., Kasteel, R., Ciocanaru, M., Herbst, M., Vereecken, H., Javaux, M., Vanclooster, M., 2002. Analytical solutions of non-linear flow and transport equations to test numerical models for simulating flow and transport in unsaturated soils. In: Marinoschi, G., (Ed.), *Proceedings of the First Workshop on Mathematical Modelling of Environmental Problems*, Bucharest, Romania, June, Publishing House of the Romanian Academy (Editura Academiei Romane), Romania.
- Vereecken, H., Maes, J., Feyen, J., Darius, P., 1989. Estimating the soil moisture retention characteristic from texture, bulk density and carbon content. *Soil Sci.* 148(6), 389–403.
- Wilson, B.N., Evaluation of hydrologic models using statistical methods. ASAE Paper 01-012207, Presented at 2001 ASAE Annual International Meeting, St Joseph, MI, 2001.
- Yeh, W.W.-G., 1986. Review of parameter identification procedures in groundwater hydrology: the inverse problem. *Water Resour. Res.* 22, 95–108.
- Zou, Z.-Y., Young, M.H., Li, Z., Wierenga, P.J., 2001. Estimation of depth averaged unsaturated soil hydraulic properties from infiltration experiments. *J. Hydrol.* 242, 26–42.